

Spin Distribution and Bonding in $[\text{Mo}(\text{OD}_2)_6]^{3+}$ Stephen P. Best,^{*,†,‡} Brian N. Figgis,[‡] J. Bruce Forsyth,[§] Philip A. Reynolds,^{‡,‡} and Philip L. W. Tregenna-Piggott[†]

Department of Chemistry, University College London, 20 Gordon Street, London WC1H 0AJ, U.K., Department of Chemistry, University of Western Australia, Nedlands, WA 6009, Australia, and ISIS Science Division, Rutherford Appleton Laboratory, Chilton, Oxon OX11 0QX, U.K.

Received April 6, 1995[⊗]

Polarized neutron diffraction results from a $\text{CsMo}(\text{SO}_4)_2 \cdot 12\text{D}_2\text{O}$ single crystal have enabled the spin distribution within the $[\text{Mo}(\text{OD}_2)_6]^{3+}$ ion to be determined with sufficient precision to permit a close examination of the metal–water bonding interactions. Most of the spin (*ca.* 90%) is concentrated in the molybdenum(III) t_{2g} orbitals, but there is significant spin transfer to the ligand. The water molecule bound to molybdenum(III) has trigonal planar coordination about the oxygen atom, and the spatial distribution of the spin about the ligand is defined with good precision. The spin about the oxygen atom is concentrated in the Mo–O interbond region ($-0.017(3) \mu\text{B}$) and in orbitals which are out of the plane of the water molecule ($0.035(5) \mu\text{B}$). A simple 10 parameter model which includes oxygen-centered sp^2 hybrid orbitals fits the 178 observations with $R_w = 0.0336$ and $\chi^2 = 1.23$. These results provide unequivocal evidence for the presence of metal–water π -bonding normal to the plane of the water molecule and the absence of significant in-plane metal–ligand spin transfer implies that metal–ligand π interaction is highly anisotropic. The anisotropy of the metal–ligand π interaction may lead to Jahn–Teller distortions in cases where there is uneven occupancy of the t_{2g} orbitals.

In contrast to the well-established examples of Jahn–Teller distortions resulting from uneven occupancy of the metal e_g (O_h) orbitals,¹ there are few such examples which involve the t_{2g} orbitals. The differing behavior is unsurprising and is related to the non- π -bonding character of the t_{2g} orbitals.² Owing to the relative weakness of the metal–ligand π interaction in electrovalent transition-metal complexes, Jahn–Teller effects involving the t_{2g} orbitals ought to be most evident in cases where the orbital degeneracy is lifted without altering significantly the M–L σ interactions. This requirement is satisfied when the ligand has nonequivalent π orbitals. In this case the degeneracy of the metal t_{2g} orbitals may be lifted by a concerted rotation of the ligand about the M–L bond. Such ligands may be designated π anisotropic, and examples include heterocyclic aromatic molecules such as pyridine or simple molecules such as nitrite or water (when the geometry about the coordinating atom is trigonal planar). Our research in this area has focused on the case where water is the ligand, this being based on the wide range of homoleptic divalent and trivalent transition metal aqua ions which are isolable and amenable to experimental study. However, it should be noted that in such cases structural characterization requires high quality neutron diffraction data, and in addition, the interpretation needs to account for the effects of hydrogen bonding.

The importance of electronic effects on the stereochemistry of water coordination is suggested by observations relating the geometry of the complex to the electron count. For example,

the d^1 cation, $[\text{Ti}(\text{OH}_2)_6]^{3+}$, exhibits *all-vertical* D_{3d} symmetry,³ and the d^2 cation, $[\text{V}(\text{OH}_2)_6]^{3+}$, exhibits *all-horizontal* D_{3d} symmetry.⁴ In both cases the geometry about the coordinating oxygen atom is trigonal planar and, for a π -anisotropic ligand, the geometry of the complex gives the maximum splitting of the orbitals which comprise the t_{2g} set. Further, provided that the M–L π interaction is greater in the plane normal to the water molecule, both complexes give orbital singlet ground terms. A range of accurate neutron structures are available for trivalent hexaaqua cations in the cesium alum lattice.^{5–8} In this lattice the trivalent cation lies on a site of S_6 symmetry and the orientation of the plane of the coordinated water molecule is largely determined by the hydrogen bonding requirements of the crystal, and this is found to be intermediate between that required for T_h and *all-horizontal* D_{3d} symmetry. In cases where there is uneven occupancy of the t_{2g} orbitals there is a small but significant distortion of the structure toward *all-horizontal* D_{3d} symmetry.⁶ Perhaps the most clear indication of the importance of electronic considerations on the structural chemistry is the observation that trivalent cations which have uneven occupancy of the t_{2g} orbitals (Ti^{III} , V^{III} and Ru^{III}) are only known to give β -alums^{9,10} whereas similarly sized trivalent cations which have even occupancy of the t_{2g} orbitals give both α - and β -alums according to the relative sizes of the other ions

[†] University College London.[‡] University of Western Australia.[§] Rutherford Appleton Laboratory.[‡] Present Address: School of Chemistry, University of Melbourne, Parkville, Victoria 3052, Australia.[‡] Present address: Research School of Chemistry, Australian National University, Canberra, ACT 0200, Australia.[⊗] Abstract published in *Advance ACS Abstracts*, August 1, 1995.

- (1) Lever, A. B. P. *Inorganic Electronic Spectroscopy*, 2nd ed.; Elsevier: Amsterdam, 1984.
- (2) Huheey, J. E.; Keiter, E. A.; Keiter, R. L. *Inorganic Chemistry: Principles of Structure and Reactivity*, 4th ed.; Harper Collins: New York, 1993; pp 449–453.

- (3) Cotton, F. A.; Fair, C. F.; Lewis, G. E.; Mott, G. N.; Ross, F. K.; Schultz, A. J.; Williams, J. M. *J. Am. Chem. Soc.* **1984**, *106*, 3519.
- (4) Tachikawa, H.; Ichikawa, T.; Yoshida, H. *J. Am. Chem. Soc.* **1990**, *112*, 977.
- (5) Best, S. P.; Forsyth, J. B.; Tregenna-Piggott, P. L. W. *J. Chem. Soc., Dalton Trans.* **1993**, 2711–2715.
- (6) Best, S. P.; Forsyth, J. B. *J. Chem. Soc., Dalton Trans.* **1991**, 1721–1725.
- (7) Best, S. P.; Forsyth, J. B. *J. Chem. Soc., Dalton Trans.* **1990**, 3507–3511.
- (8) Best, S. P.; Forsyth, J. B. *J. Chem. Soc., Dalton Trans.* **1990**, 395–400.
- (9) Haussühl, S. Z. *Kristallogr., Kristallgeom., Kristallphys., Kristallchem.* **1961**, *116*, 371.
- (10) Beattie, J. K.; Best, S. P.; Del Favero, P.; Skelton, B. W.; Sobolov, A. N.; White, A. H. Manuscript in preparation.

in the lattice. A key factor in the interpretation of these observations is the anisotropy of the M–L π interaction. While metal–water bonding has been examined by theoretical methods,^{11–13} it is important to extend the experimental measurements so as to more clearly define the characteristics of the interaction. In this report the anisotropy of the metal–water π interaction is examined directly by polarized neutron diffraction techniques.

The spin distribution within paramagnetic transition-metal complexes is a key source of information on metal–ligand bonding. Experimentally, the spin distribution may be obtained indirectly from analysis of the hyperfine couplings of the ESR spectra¹⁴ or, more directly, from magnetic structure factors obtained by single crystal polarized neutron diffraction (PND).^{15,16} A number of PND studies are available for divalent metal hexaaqua ions, and have shown covalent effects in spin transfer amounting to *ca.* 5% of the total spin density.^{17–21} However, no study of a trivalent metal hexaaqua ion has yet been reported. Since the extent of covalence is expected to be greater for such a more highly charged ion, the magnitude of spin transfer to the water molecule may be increased, and different models of the covalent interaction may be better evaluated. This advantage is further enhanced for second- or third-row transition-metal ions, since in these cases the greater radial extent of the 4d and 5d orbitals also leads to stronger covalent interaction. Molybdenum(III) is therefore a prime candidate for a PND-based examination of metal–water bonding since, in addition to the factors described above, its d^3 electron configuration results, for octahedral complexes, in a spin quartet ground term with minimal orbital contribution to the magnetic moment ($^4A_{2g}$). Despite its oxidative instability, the $[\text{Mo}(\text{OD}_2)_6]^{3+}$ cation is stabilized in the cesium alum lattice, which additionally provides a near-octahedral symmetry site with a single crystallographically unique water molecule in its first coordination sphere.

Experimental Section

The preparation of $\text{CsMo}(\text{SO}_4)_2 \cdot 12\text{D}_2\text{O}$ has been described previously.⁵ The crystal used for the PND measurements was the same as that employed for the structural determination. Since the wavelength used for the structure determination (0.8344 Å) was similar to that for the present study, the parameters describing the small extinction observed there are also appropriate for correction of this PND data.

PND measurements were made using the D3 diffractometer at the Institut Laue-Langevin, Grenoble, France, at a wavelength of 0.8430 Å obtained from a Heusler alloy monochromator. The 41 mg sample was maintained in a field of 4.62(1) T along [110] and at a temperature of 1.63(3) K. The flipping ratios of a total of 679 reflections were obtained out to $(\sin \theta)/\lambda = 0.6 \text{ \AA}^{-1}$ for reflections with h, k, l all even or all odd, and out to 0.3 \AA^{-1} for the remaining "mixed" reflections. A standard reflection was examined after every 20 measurements. The

flipping ratios, together with the nuclear structure factors, based on the previously determined low-temperature structural parameters,⁵ permit calculation of the magnetic structure factors.²² After averaging results for equivalent reflections, a total of 198 independent magnetic structure factors were obtained. Previous PND results suggest that in cases where either the flipping ratio lies far from unity ($< 1/2$ or > 2), or the nuclear structure factor is low ($F_N(hkl) < 20 \text{ fm}$), there may be large errors in the magnetic structure factors.¹⁶ Accordingly, six and 12 reflections, respectively, were rejected. An additional four reflections were rejected which had F_M values seriously out of line with any modelling of the data. Closer inspection of these reflections showed that in each case the F_N values were small ($< 4 \times 10^{-14} \text{ m}$), and either the F_M value was derived from a single measurement or else there was poor agreement between the equivalent measurements.

The applied magnetic field along [110] makes angles of 90 or 35.5° with the crystallographic 3-fold axes of symmetry passing through the four molybdenum atoms in the cubic unit cell, and that, owing to the small anisotropy of the g values ($g_{\parallel} = 1.954$, $g_{\perp} = 1.950^{23}$), results in the two pairs of trivalent cations having nonequivalent magnetizations. This lowers the unit cell symmetry and leads to nonequivalence of reflections equivalent in unpolarized nuclear scattering. For reflections of the type $h, k = 2n, l = 2n' + 1$ or $h, k = 2n + 1, l = 2n'$, there is a spherical (j_0) component in the scattering which is otherwise very small for other reflection types. While in a small number of cases there was poor agreement between nuclear equivalent reflections with mixed even/odd induces prior to merging, no systematic effect of the form described above was evident in the data.

In order to provide an estimate of the magnetization of the sample under the conditions of the PND experiment, magnetization measurements were carried out at low temperatures (2–9 K) and high field strengths (2–5 T). These were obtained using a SQUID magnetometer. Under the conditions of the experiment $\text{CsMo}(\text{SO}_4)_2 \cdot 12\text{D}_2\text{O}$ remains cubic and measurements were conducted on a 95 mg polycrystalline sample.

The 177 observed magnetic structure factors (including $F_M(000)$ obtained from magnetization measurements) were used as input data to the least-squares refinement program ASRED,^{24,25} which has the option of refining the magnetization density in terms of the populations of nuclear-centered valence orbitals. Given the aim of extracting chemical information from the experiment we favor this over the more general approach based on a nuclear-centered multipole expansion.²⁶ A multipole fit, to the same order at each site, requires seven more parameters and is an overparametrization of the data. Taking the 3-fold axis of the $[\text{Mo}(\text{OD}_2)_6]^{3+}$ cation as the z -axis of quantization for the molybdenum atom, the Mo^{III} 4d atomic orbitals are represented by the functions $e_g(\sigma)$, $e_g(\pi)$ and a_g ; the scattering from these one-electron density functions is evaluated using a series of spherical harmonics and the Fourier transform of the Hartree–Fock 4d radial distribution function.²⁴ All form factors for the valence orbitals of the Mo^{III} , O, and D atoms were obtained by Fourier transformation of the best available wave functions.²⁷ The $e_g(\pi)$ and a_g functions correlate with the t_{2g} (O_h) orbitals and $e_g(\sigma)$ correlates with e_g (O_h). The spin distribution about the oxygen atom was modeled using either 2s, sp^2 , or sp^3 orbital sets. For the latter two cases, the x axis of quantization was taken to be along the O–Mo bond, with z perpendicular to the water molecule plane. The distribution about the deuterium atoms was modeled by 1s orbitals. To minimize the number of parameters used in the refinement, the parameters for the two crystallographically inequivalent deuterium atoms were constrained to be the same, as were the populations of the oxygen-based functions directed at the deuterium atoms. The similarity of the O–D bond lengths⁵ is consistent with this restriction.

- (11) Tachikawa, H.; Ichikawa, T.; Yoshida, H. *J. Am. Chem. Soc.* **1990**, *112*, 982.
 (12) Chandler, G. S.; Christos, G. A.; Figgis, B. N.; Gribble, D. P.; Reynolds, P. A. *J. Chem. Soc., Faraday Trans.* **1992**, *88*, 1953–1959.
 (13) Åkesson, A.; Pettersson, L. G. M.; Sanström, M.; Wahlgren, U. *J. Am. Chem. Soc.* **1994**, *116*, 8691.
 (14) Getz, D.; Silver, B. L. *J. Chem. Phys.* **1974**, *61*, 630.
 (15) Wedgwood, F. A. *Proc. R. Soc. London, A* **1976**, *349*, 447.
 (16) Figgis, B. N.; Forsyth, J. B.; Reynolds, P. A. *Inorg. Chem.* **1987**, *26*, 101–105.
 (17) Deeth, R. J.; Figgis, B. N.; Forsyth, J. B.; Kucharski, E. S.; Reynolds, P. A. *Proc. R. Soc. London, A* **1989**, *421*, 153–168.
 (18) Figgis, B. N.; Forsyth, J. B.; Kucharski, E. S.; Reynolds, P. A.; Tasset, F. *Proc. R. Soc. London, A* **1990**, *428*, 113–127.
 (19) Fender, B. E. F.; Figgis, B. N.; Forsyth, J. B. *Proc. R. Soc. London, A* **1986**, *404*, 139–145.
 (20) Fender, B. E. F.; Figgis, B. N.; Forsyth, J. B.; Reynolds, P. A.; Stevens, E. *Proc. R. Soc. London, A* **1986**, *404*, 127–138.
 (21) Delfs, C. D.; Figgis, B. N.; Forsyth, J. B.; Kucharski, E. S.; Reynolds, P. A.; Vrtis, M. *Proc. R. Soc. London, A* **1992**, *436*, 417–436.

- (22) Brown, P. J.; Forsyth, J. B.; Mason, R. *Phil. Trans. R. Soc. London* **1980**, *B290*, 241.
 (23) Jacobsen, C. J. H.; Pedersen, E. *Inorg. Chem.* **1991**, *30*, 4477.
 (24) Figgis, B. N.; Kucharski, E. S.; Williams, G. A. *J. Chem. Soc., Dalton Trans.* **1980**, 1515.
 (25) Figgis, B. N.; Reynolds, P. A. *Inorg. Chem.* **1985**, *24*, 1864.
 (26) Hansen, N. K.; Coppens, P. *Acta Crystallogr.* **1978**, *A34*, 909.
 (27) Clementi, E.; Roetti, C. *At. Data Nucl. Data Tables* **1974**, *14*, 177.

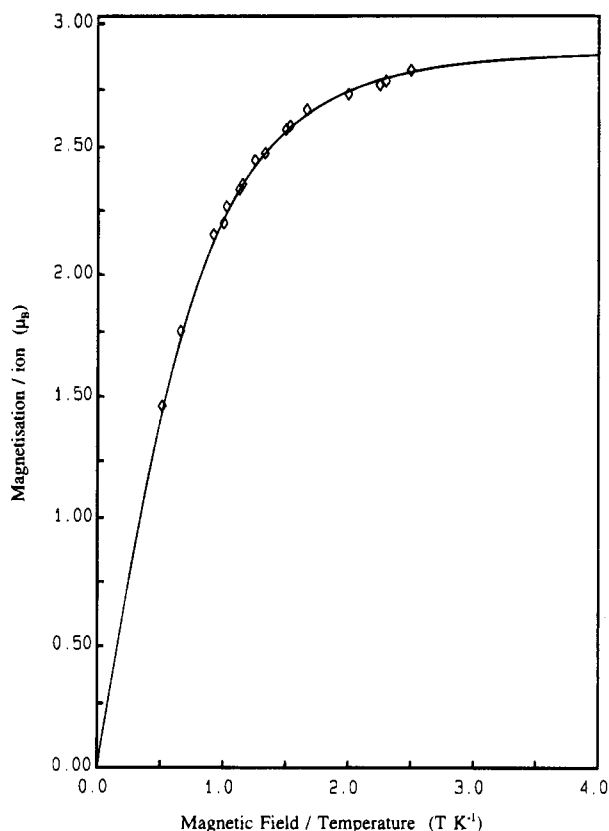


Figure 1. Magnetization of a 95 mg polycrystalline sample of $\text{CsMo}(\text{SO}_4)_2 \cdot 12\text{D}_2\text{O}$. The solid line corresponds to the Brillouin function calculated for $g = 1.951$, $J = 3/2$, and a scaling factor of 2.88.

Results and Discussion

Despite the high value of the zero field splitting parameter for the ${}^4A_{2g}$ term (1.2 cm^{-1})^{23,28} of $[\text{Mo}(\text{OH}_2)_6]^{3+}$, the experimental dependence of the magnetization on field strength and temperature fit well to a Brillouin function with $g_{\text{av}} = 1.951$ (from ESR measurements²³) and an independent scale factor (Figure 1). Thus, the Brillouin function permits a good estimate of the dependence of the magnetization of the sample on field strength and temperature under conditions close to those of the PND experiment and also provides a value for the saturation magnetization ($11.52 \mu_B$). From the SQUID measurements we estimate that the magnetization per unit cell of $\text{CsMo}(\text{SO}_4)_2 \cdot 12\text{D}_2\text{O}$ at 4.62(1) T and 1.63(3) K is $11.33 \mu_B$. This is 98.4% of the saturation magnetization. It should be noted that measurements of the magnetization, while precise, may be systematically low owing to the oxidative instability of the sample. If this is so, a better value for $F_M(000)$ may be estimated as $11.51 \mu_B$ based on the g_{av} value obtained from ESR measurements and use of the Brillouin function (Figure 1). All models described below were refined using the $F_M(000)$ value derived from direct measurement ($11.33 \mu_B$). The use of the higher calculated $F_M(000)$ value of $11.51 \mu_B$ most strongly affects the population of the most radially diffuse functions, *i.e.* the Mo 5s orbital; however, for each of the models the resultant shift in the calculated population of this orbital was less than 1 esd.

The coordination geometry about the Cs^+ cation has been shown to provide a clear distinction between the different alum types,²⁹ with the O(a)CsO(a) angle of 60.0° found for $\text{CsMo}(\text{SO}_4)_2 \cdot 12\text{D}_2\text{O}$ ^{5,30} being typical for the β modification. The molybdenum(III) cations lie on sites of S_6 symmetry within the

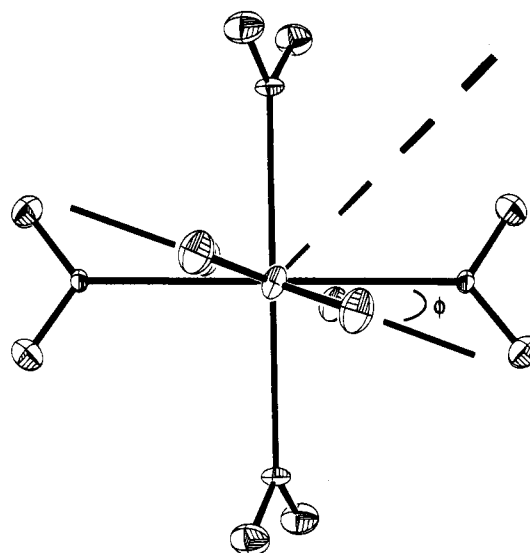


Figure 2. View of the $[\text{Mo}(\text{OD}_2)_6]^{3+}$ cation with the 3-fold symmetry axis (dashed line) in the front-top-right quadrant. In this arrangement ϕ is defined as the angle between the plane of the water molecule and the horizontal plane defined by the metal atom and four of the oxygen atoms.

$Pa\bar{3}$ cubic unit cell. The MoO_6 octahedron is almost regular (OMO angle = 91.1°) and is inclined by 0.78° to the unit cell axes. The trivalent cations are well separated within the lattice with a Mo–Mo separation of 8.79 Å. The water molecule coordinated to molybdenum(III) defines a plane which makes an angle of $1.8(1)^\circ$ to the Mo–O bond vector. The orientation of the plane of the water molecule relative to the MoO_6 framework is shown in Figure 2. The angle between the plane of the water molecule and the horizontal plane (defined with the 3-fold axis in the front-top-left octant of the octahedron), ϕ ,⁵ is $-19.7(1)^\circ$. Strong hydrogen bonds between the water molecules coordinated to the trivalent cation and the sulfate groups and the remaining water molecules provide the link between the coordination geometry about the trivalent and univalent cations and the alum type. While the range of Cs–O bond lengths observed in the cesium sulfate β -alum lattice (3.298–3.359 Å to water, 3.529–3.460 Å to sulfate) reflects a limited flexibility of the coordination sphere about the cesium cation to respond to preferred orientations of the plane of the water molecule coordinated to M^{III} , the coordination geometry of the trivalent cation is largely constrained by the lattice. In the present case there is even occupancy of the metal t_{2g} orbitals and the orientation of the plane of the water molecule coordinated to Mo^{III} is indistinguishable from that found for the corresponding alums of trivalent cations which also have even occupancy to the t_{2g} orbitals (Cr^6 and Fe^8).

The face-centered cubic arrangement of the molybdenum(III) cations and the close alignment of the axes of the MoO_6 species with those of the unit cell permit a simple initial qualitative analysis of the PND results. For the face-centered cubic (fcc) lattice “mixed” nuclear reflections are systematically absent, and so the spherical component of the spin centered on the molybdenum(III) cation makes no contribution to the magnetic structure factors (Figure 2). For the fcc-allowed reflections the extent of interaction of the scattered neutron with the unpaired electrons of the t_{2g} orbitals can be deduced from the orientation of the scattering vector relative to the O_h axes and the scattering angle. For example, when the scattering

(29) Beattie, J. K.; Best, S. P.; Skelton, B. W.; White, A. H. *J. Chem. Soc., Dalton Trans.* **1981**, 2105–2111.

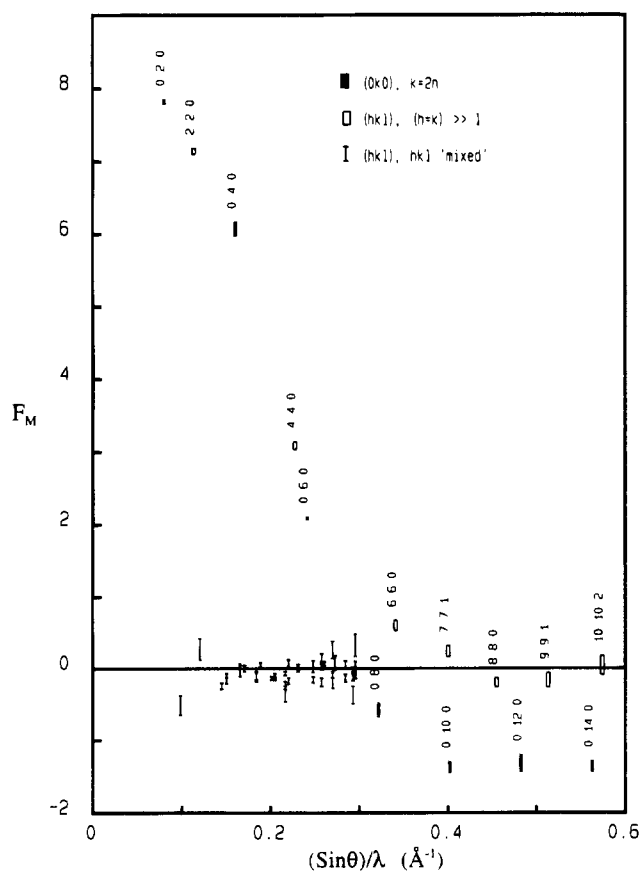
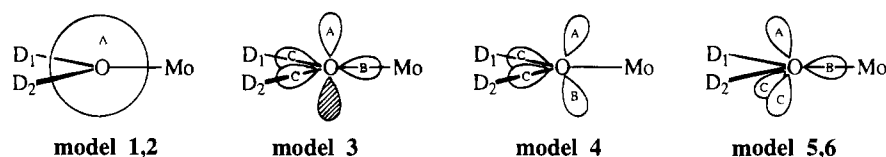
(30) Brorson, M.; Gajhede, M. *Inorg. Chem.* **1987**, 26, 2109.

(28) Krausz, E. *Aust. J. Chem.* **1993**, 46, 1041–1054.

Table 1. Magnetization Populations Obtained from Fitting the PND Results of $\text{CsMo}(\text{SO}_4)_2 \cdot 12\text{D}_2\text{O}$ ^a

	model 1 (2s)	model 2 (2s)	model 3 (sp ²)	model 4 (sp ³)	model 5 (sp ³)	model 6 (sp ³) ^b
$e_g(\sigma)$	-0.06(3)	-0.05(3)	-0.03(2)	0.04(3)	-0.03(2)	-0.03(2)
$e_g(\pi)$	1.73(3)	1.76(3)	1.69(3)	1.75(3)	1.70(3)	1.69(3)
a_g	1.04(2)	1.07(2)	1.02(2)	1.05(2)	1.02(2)	1.03(2)
4d radial	1.071(3)	1.078(4)	1.068(4)	1.076(4)	1.069(4)	1.069(4)
5s		-0.20(4)	-0.10(4)	-0.16(4)	-0.08(4)	-0.08(4)
5s radial		1.1(1)	1.6(3)	1.1(1)	1.6(4)	1.6(5)
orbital A	0.024(2)	0.027(2)	0.035(5)	0.015(3)	0.020(3)	0.017(4)
orbital B			-0.017(3)	-0.002(4)	-0.013(3)	-0.014(3)
orbital C			0.003(2)	0.007(2)	0.010(2)	0.011(2)
$D_1(1s) = D_2(1s)$	0.002(2)	0.009(2)	0.009(2)	0.007(2)	0.006(2)	0.005(2)
R_w	0.0431	0.0382	0.0317	0.0370	0.0333	0.0336
χ^2	1.65	1.48	1.23	1.44	1.29	1.31

^a The population units are Bohr magnetons (μ_B). The values of the spin populations of the ligand orbitals are given per orbital. ^b The quantization axes for the sp³ hybrids have been selected so as to preserve a local mirror plane normal to the water molecule. The Mo–O bond vector makes an angle of 1.8° with the plane of the water molecule. In model 5 this tilt is toward orbital A, and in model 6 the tilt is in the opposite sense.

Chart 1**Figure 3.** Dependence of $F_M(hkl)$ on scattering angle for a range of selected reflections.

vector lies along the O_h axes (reflections of the type $(0k0)$), the interaction is at a maximum when the scattering angle (2θ) is 90° and a minimum when 2θ is equal to zero. This situation is reversed when the scattering vector lies between the axes ($(hk0)$ reflections). Thus, the t_{2g} character of the spin distribution about the Mo^{III} cation is shown by the rapid decrease of the $F_M(hh0)$ values of reflections with increasing scattering angle compared with that of the $(0k0)$ reflections (Figure 3). Similar behavior has previously been noted for $[\text{CrF}_6]^{3-}$ in K_2NaCrF_6 .¹⁵

The g values for the $[\text{Mo}(\text{OH}_2)_6]^{3+}$ ion doped into $\text{CsIn}(\text{SO}_4)_2 \cdot 12\text{H}_2\text{O}$ indicate almost complete quenching of the orbital angular momentum by the ligand field. Thus, the magnetization density here may be related to the spin density³¹ by a simple scale factor, and this simplifies the analysis of the PND results.

Quantitative results obtained by the refinement of six different orbital models (shown in Chart 1) are given in Table 1. In each case the observation/parameter ratio is greater than 17. For each model there is trigonal distortion of the 4d magnetization and, as is to be expected, most of the spin (*ca.* 90%) is localized in metal t_{2g} (O_h) orbitals. The fit to the experimental results using only these metal-centered functions and an isotropic function centered on the oxygen atom (model 1) is significantly improved by the addition of a diffuse Mo-centered 5s orbital (model 2). The major effect of such a term is to bring into better agreement the calculated and experimental values of $F_M(000)$. An increase in the magnitude of the negative population of this orbital leads to higher values of the spin located in the D 1s orbital and, to a lesser extent, in the oxygen-centered orbitals. When sp² or sp³ functions are used to model the spin distribution about the oxygen atom, the inclusion of the Mo 5s orbital has similar effects. A radially diffuse orbital with a negative population is found in previous PND studies of divalent metal hexaaqua cations.^{17–21} The population of the Mo 5s orbital may be significant but is sensitive to the modeling of the spin about the oxygen atom. In the cases where the spin about the oxygen is comparatively well modeled the population of the Mo 5s orbital is less than 3 esd's (−0.10(4) for model 3 and −0.08(4) for models 5 and 6). However we should note that because of the lack of low wave vector reflections in this small, highly-symmetric unit cell the population is relatively poorly defined and no experimental distinction can be made between 5s and 5p or indeed any other orbital occupations resulting in diffuse spin density.

Most of the spin distribution is described adequately using model 2, but the description fails to define the spin anisotropy about the oxygen atom, and this is critical for the definition of the molybdenum–water interaction. The most appropriate

(31) Lovesey, S. W., *Theory of Neutron Scattering from Condensed Matter*; International Series of Monographs on Physics, No. 72; Oxford University Press: Oxford, England, 1984; Vol. 2.

orbital description of the oxygen site may be either sp^2 , based on the trigonal planar coordination geometry about the oxygen atom, or sp^3 , based on the H—O—H bond angle (111.1°). The contributions to the magnetization given by model **3** (sp^2) show that the 2p orbital, which is normal to the plane of the water molecule, has a significantly greater occupation than have the two hybrid orbitals which lie in the plane and which point toward the deuterium atoms. There is also significant negative occupation of the hybrid orbital directed at the molybdenum atom. The R factor and goodness of fit obtained in this case is the best obtained of all the models examined and is a sufficient improvement on model **2** to justify the modeling of the spin anisotropy about the oxygen atom.

When sp^3 hybrid orbitals are used to model the spin density about the oxygen atom, there are choices for the directions of the quantization axes as shown for models **4–6** in Table 1. Model **4** has no hybrid orbital available to describe the significant spin density along the Mo—O bond found in the sp^2 refinement, and the χ^2 and R_w values are significantly higher than those of model **3**, and indeed are little better than those of model **2** where a single s orbital is used to model the spin on the atom. Alternatively, the oxygen atom may be treated as sp^3 hybridized with one hybrid directed along the Mo—O bond and the other three such orbitals disposed so as to preserve a local plane of symmetry normal to the plane of the water molecule. The small tilt of the plane of the coordinated water molecule relative to the Mo—O bond vector leads to two inequivalent arrangements. In model **5** the deuterium atoms are further from the pair of hybrid orbitals related by the mirror plane than in model **6**. Since the tilt of the plane of the coordinated water molecule is small (1.8°) both refinements would be expected to give similar results, as is indeed the case (Table 1). While models **5** and **6** both give a better fit of the data than model **2** in each case, the results are significantly poorer than those obtained with sp^2 hybrid orbitals on the oxygen atom. Furthermore, from a chemical perspective, models **5** and **6** are not entirely satisfactory since the hybrid orbitals bear a poor relationship to the molecular structure.

In models **3–6**, the choice and disposition of the orbitals on the oxygen atom permit description of the Mo—O π bonding normal to the plane of the water molecule but not in it. In order to examine the extent of in-plane π bonding model **3** was extended by the addition of an oxygen 2p orbital normal to the Mo—O bond and parallel to the plane of the water molecule located at (a) the oxygen atom, (b) 75% of the Mo—O bond length, and (c) the midpoint of the bond. In all three cases, the population of the additional orbital remained below the 1 esd level and the quality of the fit of the experimental data was not improved significantly. Thus, there is no experimental evidence for Mo—O π interaction in the plane of the water molecule.

A comparison of the PND results for the divalent hexaaqua cations of V,¹⁷ Cr,²¹ Mn,²⁰ Fe,¹⁸ and Ni¹⁹ in the Tutton salt lattice has been reported,¹⁷ but this is the first opportunity to make such a comparison with a trivalent cation. A direct comparison is most straightforward between the $[\text{Mo}(\text{OD}_2)_6]^{3+}$ and the $[\text{V}(\text{OD}_2)_6]^{2+}$ ions since they have the same formal valence d-electron configuration, d^3 . In the Tutton salt lattice the divalent cation occupies a site of C_i symmetry, although the local symmetry is approximately S_6 , the same as the site symmetry of the trivalent cation in the alum lattice. The mode of water coordination is trigonal pyramidal, with a 45° angle between the V^{II}—O bond vector and the plane of the coordinated water molecule. The spin distribution about the vanadium was modeled using 3d t_{2g} and 3d e_g orbitals as well as a set of 4d

t_{2g} and 4d e_g orbitals. The water molecule was modeled using sp^2 orbitals centered on the oxygen atom, with the quantization axes aligned with the V^{II}—O bond. Both of the hydrogen atoms lie equally below the plane of the sp^2 hybrid orbitals, and 1s functions were centered on the hydrogen atom. An additional feature of the PND refinements of the Tutton salts is the inclusion of a Gaussian function in the M^{II}—O interbond region. In the case of the vanadium(II) salt the population of this orbital is small ($0.010(11) \mu_B$).

Both the vanadium(II) and molybdenum(III) cations have the formal t_{2g}^3 valence electron configuration. For vanadium(II) the "observed" unpaired electron configuration is $t_{2g}^{2.84(6)}e_g^{-0.03(4)}$ and for molybdenum(III), $t_{2g}^{2.73(3)}e_g^{-0.03(2)}$. Detailed comparison is complicated by differences in the stereochemistry of the water coordination in the two cases, and the populations are barely significantly different, but if there is greater spin transfer from the metal-based orbitals for molybdenum(III) it is readily explained in terms of the greater extent of oxygen to metal charge transfer which follows from the higher charge on the metal and simple orbital overlap considerations. For molybdenum(III) the spin distribution is determined with good precision and the planar geometry of water coordination facilitates the examination of the metal—water π -bonding interaction. This is in contrast with vanadium(II) in the Tutton salt lattice where the lower site symmetry and the significant tilt of the plane of the coordinated water molecule complicate such a comparison. Indeed the earlier suggestion¹⁷ that the predominant metal—water π interaction is in the plane of the water molecule is not borne out by the present results from $[\text{Mo}(\text{OD}_2)_6]^{3+}$, where the mode of water coordination is trigonal planar.

Two features of the earlier studies of Tutton salts which are borne out by the present study are the significant positive spin population on the hydrogen atoms and the need to have oxygen-based orbitals directed along the M—O bond. The spin transfer to the deuterium atoms observed for vanadium(II) $0.015(2)$ is comparable with that found for molybdenum(III) $0.009(2)$; however it should be noted that this population is sensitive to the model used. Comparison of model **4** with either **5** or **6** give a clear indication of the importance of the spin distribution in the interbond region. It is noteworthy that a simple orbital model describes very well this aspect of the spin distribution for $\text{CsMo}(\text{SO}_4)_2 \cdot 12\text{D}_2\text{O}$.

Conclusion

The spin density in $\text{CsMo}(\text{SO}_4)_2 \cdot 12\text{D}_2\text{O}$ has been obtained by low-temperature PND studies. The quality of the data is sufficient to permit examination of the M—O bonding interactions which are of chemical interest. A molecular orbital model of metal—ligand interactions in which the water molecule is involved in both σ and π bonding, but where the π bonding is different in; and normal to the plane of the ligand fits the PND results very well. The sp^2 based-model of the magnetization density is consistent with there being more spin transfer to oxygen orbitals perpendicular to the plane of the water molecule than to orbitals lying in the plane. This feature is also apparent in the better of the sp^3 based-models. The magnetization found in the region of the Mo—O bond is opposite in sign to that in the t_{2g} orbitals, and this is indicative of electron correlation effects. In the present case the magnetization in the Mo—O interbond region is well modeled by a single oxygen-centered orbital. The oxygen is best treated as sp^2 hybridized with $0.035(5) \mu_B$ in each oxygen 2p-orbital which is normal to the plane of the water molecule and $0.003(2) \mu_B$ in the two hybrid orbitals

which lie in the plane. The Mo—O interactions in-plane and normal to the plane of the water molecule are significantly different. The anisotropy of the magnetization density about the oxygen atom is in keeping with expectations based on overlap and energy matching of the metal and ligand orbitals. The structural chemistry of the alums has been rationalized in terms of a metal—oxygen π interaction which is greatest normal to the plane of the water molecule, and which is the main contribution to the trigonal field which lifts the degeneracy of the t_{2g} orbitals.^{6,29} This proposition is supported by the analysis of the low temperature electronic spectrum of $\text{NH}_4\text{V}(\text{SO}_4)_2 \cdot 12\text{H}_2\text{O}$ which shows that the transition energies can be interpreted using the angular overlap model only if the π bonding in the plane of the water molecule is considerably weaker than that perpendicular to the plane.³²

Acknowledgment. The authors are grateful to Francis Tasset (ILL) for his unstinting efforts during the D3 experiment, and to Professor John Crangle (University of Sheffield) for his help in obtaining the bulk magnetization of our sample. We are also indebted to Sean Howard who undertook *ab initio* calculations on the $[\text{Mo}(\text{OD}_2)_6]^{3+}$ complex, and to Paul Mallinson for sharing his expertise with the charge density program MOLLY. Thanks are due to the SERC for the award of a fellowship (P.L.W.T.-P.), to UCL for study leave (S.P.B.), and to the Australian Research Council for financial support (B.N.F. and P.A.R.).

IC950401T

(32) Hitchman, M. A.; McDonald, R. G.; Smith, P. W.; Stranger, R. *J. Chem. Soc., Dalton Trans.* **1988**, 1393.